ASME WAM'91, Symposium on Heat and Mass Transfer in Solidification Processing,
Organizer: Suresh G. Advani, Atlanta, GA, December 1-6, 1991.

SOLIDIFICATION IN REDUCED GRAVITY WITH MAGNETIC FIELDS AND TEMPERATURE-DEPENDENT PHYSICAL PROPERTIES

George S. Dulikravich
Associate Professor
Aerospace Eng. Dep.
Penn State Univ.
University Park, PA

Branko Kosovic
Graduate Student
Aerospace Eng. Dep.
Penn State Univ.
University Park, PA

Seungsoo Lee
Research Scientist
Aerodynamics Dep.
Agency for Defense Dev.
Daejon, South Korea

ABSTRACT

A complete mathematical model has been developed together with an accompanying computer code for the numerical prediction of steady, viscous, laminar, incompressible flows with strong heat conduction, magnetic field effects (ponderomotive forces and Joule ating), latent heat of phase change, and thermal buoyancy. The code is capable of simultaneously predicting fluid flow field and the solidifying regions resulting from strong localized wall cooling. The formulation allows for temperature dependance of physical properties and utilizes Boussinesq approximation for thermal buoyancy. Numerical results for solidification of a silicon melt in a closed container demonstrate the influence of strong magnetic fields on the thermal buoyancy flow and consequently on the liquid/solid interface shape.

NOMENCLATURE

c_P = specific heat at constant pressure, J kg^{-1} K^{-1}

c_v = specific heat at constant volume, J kg^{-1} K^{-1}

E = electric field, V m^{-1}

Ec = Eckert number

Fr = Froude number

g = gravity force per unit volume, m s^{-2}

Gr = Grashof number

H = magnetic field, H kg^{-1}

Ht = Hartmann number

J = electric current density, A m^{-2}

k = heat conductivity coefficient, W m^{-1} K^{-1}

l = length, m

L = latent heat of liquid/solid phase change, J kg^{-1}

Mm = magnetic Mach number (Mm^2 = ReRm/Ht^2)

p = pressure, kg m^{-1} s^{-2}

Pm = magnetic Prandtl number

Pr = Prandtl number

Re = hydrodynamic Reynolds number

Rm = RePm = magnetic Reynolds number

S = volume fraction of the liquid phase

t = time, s

T = absolute temperature, K

$\Delta T_o = T_h - T_c$ = temperature difference, K

v = (u,v,w) = velocity vector, m s^{-1}

x,y,z = cartesian coordinates, m

α = thermal expansion coefficient, K^{-1}

θ = nondimensional temperature

ρ = density, kg m^{-3}

η = coefficient of shear viscosity, kg m^{-1} s^{-1}

ζ = coefficient of secondary viscosity, kg m^{-1} s^{-1}

μ = magnetic permeability, H m^{-1}

σ = electrical conductivity, Ω^{-1} m^{-1}

ϕ = nondimensional gravity potential

Φ = viscous dissipation function, kg m^{-1} s^{-3}

subscripts

c = cold wall

h = hot wall

o = reference values

s = solidus

l = liquidus

superscripts

* = nondimensional values

' = function of nondimensional temperature

INTRODUCTION

The numerical study conducted and presented in this work involves the phase change process. This process is of crucial interest in the problems of casting, rystallization or freezing of living tissues. Although deeper insight in the given phenomena has already been acquired, the application of theoretical achievements is still not satisfactory. Serious limitations are set by the current state of numerical methods and available computing hardware. From the computational point of view, to efficiently solve a phase change problem in a multidimensional domain still represents a challenging task [1,2]. A summary of most of the commonly used analytical and numerical models [3] indicates a need for further research in this area. An analytical solution for the phase change problem exists only for the one-dimensional case (Stefan's problem). The extreme importance of the aforementioned processes in technology makes a numerical simulation approach crucial for obtaining optimal characteristics of molds, crystal properties, etc. and leads to improvements in design, production technology, production control, production cost, quality of products and performance of these products.

Understanding the individual effects of a magnetic field on a fluid flow and its temperature field is crucial to numerous applications. It is known [4,5] that a magnetic field can eliminate vorticity from a flow field, while an electric field can enhance it. For example, a Poiseuille velocity profile flattens due to an applied transverse magnetic field. In the presence of a magnetic field, the strengths of vortices produced by thermal instability can be reduced.

In this work, attention will be restricted to MHD flows with a strong applied magnetic field and a negligible applied electric field [6]. The objective is to examine the recirculating flow patterns resulting from the influence of the applied magnetic field in the case of strong temperature gradients due to imposed thermal boundary conditions [7,8,9]. If the temperature of the boundary is below solidus temperature for the given material in a liquid domain, or if the temperature is above liquidus temperature for initially solid domain, a phase change in the material under consideration takes place. In this work, only the solidification process will be presented although the mathematical model as well as the computer code are general and can be used to simulate the reverse process of melting.

The applied magnetic field can be oscillatory, travelling or steady. The problem is formulated as time-dependent. Nevertheless, computational results presented in this work will concentrate on steady state situations only.

Although phase change is inherently a time dependent process, the steady state case is of great importance, too. In continuous casting or crystal growth techniques such as the Czochralski process where a fluid portion of the material undergoing phase change is always present, phase change is essentially a steady process. In these cases the shape of the solidified layer and heat transfer in the region between solid and liquid phase, commonly called the mushy region, are of special interest. From parameters obtained through steady state analysis, structural characteristics, which define the quality of the product, can be defined.

Earlier attempts to simulate magnetohydrodynamic phenomena in solidification numerically had several limitations. Very often Maxwell's equations were not solved as it was pointed out in an excellent survey article by Tseng [2]. The magnetic field was often assumed to be independent of the fluid flow field and results were obtained by simple superposition. More precisely, the influence of the magnetic field is usually introduced through source terms in the momentum equation only, while its influence on the energy equation is neglected. As it will be shown later, coupling of the fluid flow field and

the magnetic field cannot be assumed as linear and therefore it is not additive Very often the influence of the fluid motion on the magnetic field is neglected, while it is taken into account when the induced electric current computed.

In the present work, a complete three-dimensional mathematical model for laminar, steady magnetohydrodynamic flow with phase change and variable material properties is presented. A computer code was developed and numerical analysis was performed for two-dimensional cases only. At first a mathematical model of magnetohydrodynamics is presented. The electric field vector is eliminated from the Maxwell's equations using Ohm's law. This results in magnetic transport equations, which are of mixed hyperbolic-parabolic type, with mathematical character similar to the Navier-Stokes equations. Magnetic transport equations are integrated along with the Navier-Stokes equations. Sets of equations governing fluid flow and magnetic field are integrated in an alternating fashion [5].

The goal is to model and computationally simulate the magnetohydrodynamic flow of a fluid undergoing phase change. Steady flows with heat transfer and strong superimposed magnetic fields will be analyzed. The effects of a magnetic field on the fluid flow will be presented by source terms in the momentum equation (ponderomotive force) and in the energy equation (Joule heating). Thermally induced buoyancy is accounted for via the Boussinesq approximation, which is justified for the case of temperature-dependent material properties [10]. The latent heat of phase change (solidification/melting) will be incorporated applying the so-called enthalpy method [3].

It should be pointed out that due to the lack of experimental data it was not possible to rigorously validate the accuracy of the computer code. A possible reason for the scarcity of experimental data is the complexity of the problem which in order to give valuable results has to be approached simultaneously from different points of view (fluid flow measurements, magnetic field measurements, and heat transfer measurements). For some simple cases, like the so-called Hartman flow (duct flow under the influence of magnetic field) where an analytical solution exists, the validation of a simpler version of the model without phase change effects and without variable material properties has been done previously [5] demonstrating that the basic code is ighly accurate. The present work presents an extension of this recent effort and utilizes the modified version of the original software.

In order to use an incompressible laminar flow model, we have utilized the Boussinesq approximation to account for the thermal buoyancy force. Furthermore, coefficients of viscosity, heat conduction, and specific heat were allowed to vary with temperature arbitrarily. In actual examples, the physical properties including latent heat of solidification were specified as varying linearly within the narrow temperature region between solidus and liquidus. The computing logic used in this work predicts both the flow field and the accrued solid simultaneously, thus capturing the solid/liquid interface configuration without any special front tracking algorithm. In other words, the full Navier-Stokes equations (with extended Boussinesq approximation) and magnetic field transport equations [5,6,9] were iteratively solved at every point of the computational domain, except that the velocity components and their derivatives were explicitly set to zero at every point where the instantaneous temperature is lower than the solidus temperature.

ANALYTICAL MODEL

After ignoring the electric displacement vector [3], Maxwell's equations can be written in Cartesian tensor notation as:

$$H_{i,i} = 0 \qquad i = 1,2,3 \tag{1}$$

$$J_i = \varepsilon_{ijk} H_{k,j} \tag{2}$$

$$H_{i,t} = -\frac{1}{\mu} \varepsilon_{ijk} E_{k,j}. \tag{3}$$

The relationship between an induced electric current, J_i, an electric field, E_i, and a magnetic field, H_i, in a moving media is given by

$$J_i = \sigma \left(E_i + \mu \varepsilon_{ijk} v_j H_k \right) \tag{4}$$

By taking the curl of this equation (with electrical conductivity and magnetic permeability as constants) the following expression is obtained after using equation (2)

$$\varepsilon_{ijk} E_{k,j} = \frac{1}{\sigma} \varepsilon_{ijk} \left(\varepsilon_{klm} H_{l,m} \right)_{,j} - \mu \varepsilon_{ijk} \varepsilon_{klm} \left(v_l H_m \right)_{,j} \tag{5}$$

Using identity

$$\varepsilon_{ijk}\left(\varepsilon_{klm}\,H_{l,m}\right)_{,j} = \left(H_{j,j}\right)_{,i} - H_{i,jj} \tag{6}$$

and noticing that magnetic field is solenoidal, $H_{i,i} = 0$, from equations (1-3) we can derive the magnetic transport equation in the form

$$H_{i,t} - \varepsilon_{ijk}\,\varepsilon_{klm}\left(v_l\,H_m\right)_{,j} = \frac{1}{\mu\sigma}\,H_{i,jj} \tag{7}$$

or

$$H_{i,t} - \left(v_j\,H_i - v_i\,H_j\right)_{,j} = \frac{1}{\mu\sigma}\,H_{i,jj} \tag{8}$$

Only incompressible fluid flow will be considered in this work. At the same time important physical phenomena such as buoyancy forces cannot be neglected. In order to take into account the effects of buoyancy, the Boussinesq approximation will be introduced. It will be shown that the Boussinesq approximation is valid even when fluid properties vary as a function of temperature [10]. The final analytical model will be derived by starting from the full Navier-Stokes equations for a compressible fluid flow under the influence of an externally applied steady magnetic field [5,6].

$$\rho_{,t} + \left(\rho v_i\right)_{,i} = 0 \tag{9}$$

$$\left(\rho v_i\right)_{,t} + \left(\rho v_i v_j\right)_{,j} = -p_{,i} + \left(\tau_{ij}\right)_{,j} + \mu\,\varepsilon_{ijk}J_jH_k - \rho g_i \tag{10}$$

where $\mu\,\varepsilon_{ijk}J_jH_k$ is the ponderomotive force due to magnetic field and tensor τ_{ij} is the viscous stress tensor:

$$\tau_{ij} = \eta\left(v_{i,j} + v_{j,i}\right) + \zeta\,v_{k,k}\,\delta_{ij} \tag{11}$$

The energy conservation equation is given as

$$\left(\rho c_v T\right)_{,t} + \left(\rho c_v v_i T\right)_{,j} = -p\,v_{i,i} + \left(kT_{,i}\right)_{,i} + \frac{J_iJ_i}{\sigma} + \tau_{ij}\,v_{i,j} \tag{12}$$

where $\tau_{ij}\,v_{i,j} = \Phi$ is the viscous dissipation function and $\frac{J_iJ_i}{\sigma}$ is the Joule heating resulting from the induced electric current. Density , coefficients of specific heat, viscosity and heat conduction can be expressed as general functions [10] of temperature

$$\rho = \rho_o\,\rho'(\theta) \qquad c_p = c_{po}\,c_{po}'(\theta) \qquad c_v = c_{vo}\,c_{vo}'(\theta)$$

$$\eta = \eta_o\,\eta'(\theta) \qquad \zeta = \eta_o\,\zeta'(\theta) \qquad k = k_o\,k'(\theta) \tag{13}$$

where the primed values denote functions of non-dimensional temperature, θ. The entire set of partial differential equations can be non-dimensionalized by introducing the relations

$$v_i^* = \frac{v_i}{v_o} \qquad x_i^* = \frac{x_i}{l_o} \qquad t^* = \frac{t\,v_o}{l_o} \qquad p^* = \frac{p}{\rho_o\,v_o^{\,2}} \tag{14}$$

$$H_i^* = \frac{H_i}{H_o} \qquad \theta = \frac{\Delta T}{\Delta T_o} \qquad e^* = \frac{e}{c_{po}\,\Delta T_o} \qquad g^* = \frac{g_i}{g} \tag{15}$$

so that $\Delta T = T - T_c$, and $\Delta T_o = T_h - T_c$. Then, the conservation laws in non-dimensional form become

$$\rho'_{,t} + \left(\rho'\,v_i^*\right)_{,i} = 0 \tag{16}$$

$$\left(\rho' v_i^*\right)_{,t} + \left(\rho' v_i^* v_j^*\right)_{,j} = -\,p^*_{,i} + \frac{1}{Fr^2}\,\rho'\,g_i^* + \frac{1}{Re}\left[\eta'\left(v^*_{i,j} + v^*_{j,i}\right)\right]_{,j} + \frac{1}{Re}\left(\zeta'\,v^*_{j,j}\right)_{,i} + \frac{1}{Mm^2}\,\varepsilon_{ijk}\,\varepsilon_{jlm}H^*_{m,l}H^*_k \tag{17}$$

$$\left(\rho' e^*\right)_{,t} + \left(\rho' e^*\,v_i^*\right)_{,i} = \frac{1}{RePr}\left(k'\,\theta_{,i}\right)_{,i} - Ec\,p^*\,v^*_{i,i} + \frac{Ec}{Mm^2\,Rm}\,\varepsilon_{ijk}\varepsilon_{ilm}H^*_{k,j}H^*_{m,l} + \frac{Ec}{Re}\,\Phi^* \tag{18}$$

$$H^*_{i,t} - \left(v_j^*\,H_i^* - v_i^*\,H_j^*\right)_{,j} = \frac{1}{Rm}\,H^*_{i,jj} \tag{19}$$

The non-dimensional density ρ' can be expanded in a Taylor series while retaining only the first order term,

$$\rho' = 1 - \alpha^* \theta = 1 - \alpha \Delta T_o \qquad (20)$$

where

$$\alpha^* = \frac{\partial \rho'}{\partial \theta} = \frac{\Delta T_o \rho_o}{\rho_o \Delta T_o} \frac{\partial \rho'}{\partial \theta} = \frac{\Delta T_o}{\rho_o} \frac{\partial \rho}{\partial T} = \Delta T_o \alpha. \qquad (21)$$

Mass conservation then becomes

$$\left(1-\alpha^*\theta\right)_{,t} + \left[\left(1-\alpha^*\theta\right) v_i^*\right]_{,i} = 0 \qquad (22)$$

Introducing (20) in (17), the momentum equations can be written as

$$\left[\left(1-\alpha^*\theta\right) v_i^*\right]_{,t} + \left[\left(1-\alpha^*\theta\right) v_i^* v_j^*\right]_{,j} = \frac{1}{Re}\left[\eta'\left(v_{i,j}^* + v_{j,i}^*\right)\right]_{,j} + \frac{1}{Re}\left(\zeta' v_{j,j}^*\right)_{,i} - p_{,i}^* + \frac{1}{Fr^2}\left(1-\alpha^*\theta\right) g_i^* + \frac{1}{Mm^2} \varepsilon_{ijk}\varepsilon_{jlm} H_{m,l}^* H_k^* \qquad (23)$$

and the energy conservation becomes

$$\left[\left(1-\alpha^*\theta\right) e^*\right]_{,t} + \left[\left(1-\alpha^*\theta\right) e^* v_i^*\right]_{,i} = \frac{1}{RePr}\left(k' \theta_{,i}\right)_{,i} - Ec\, p^* v_{i,i}^* + \frac{Ec}{Mm^2\, Rm} \varepsilon_{ijk}\varepsilon_{ilm} H_{k,j}^* H_{m,l}^* + \frac{Ec}{Re} \Phi^* \qquad (24)$$

Since $de^* = \left.\frac{\partial e^*}{\partial \theta}\right|_{\rho'} d\theta + \left.\frac{\partial e^*}{\partial \rho'}\right|_{\theta} d\rho'$ and $\rho' = 1 - \alpha^*\theta$, then if $\left(\alpha^*\theta\right) \ll 1$ it follows that

$\left.\frac{\partial e^*}{\partial \rho'}\right|_{\theta} \approx 0$. Thus, $de^* = \left.\frac{\partial e^*}{\partial \theta}\right|_{\rho'} d\theta = c_p' \, d\theta = dh^*$, where

c_p' is not necessarily a constant.

If α^* is constant then

$$\alpha_{,t}^* = 0, \qquad \text{and} \qquad v_i \alpha_{,i}^* = 0 \qquad (25)$$

Since $\alpha^* \ll 1$, terms such as

$\alpha^* \theta_{,t}$; $v_i \alpha_{,i}^* \theta$; $\alpha^* v_i \theta_{,i}$; $\alpha^* \left(\theta e^*\right)_{,t}$;

$\alpha^* v_i \left(\theta e^*\right)_{,i}$; $\alpha^* \left(\theta v_i^*\right)_{,t}$; $\alpha^* v_i \left(\theta v_i^*\right)_{,i}$

tend to zero for moderate changes of non-dimensional temperature θ in time and space. According to the Boussinesq approximation, buoyancy force terms which are a function of $\alpha^*\theta$ cannot be neglected. Thus, the system of equations (16-19) can be reduced to

$$v_{i,i}^* = 0 \qquad (26)$$

$$v_{i,t}^* + \left(v_i^* v_j^*\right)_{,j} = \frac{1}{Re}\left(\eta' v_{i,j}^*\right)_{,j} - p_{,i}^* + \frac{1}{Fr^2} g_i^* - \frac{\alpha^*\theta}{Fr^2} g_i^* + \frac{1}{Mm^2} \varepsilon_{ijk}\varepsilon_{jlm} H_{m,l}^* H_k^* \qquad (27)$$

$$\left(c_p' \theta\right)_{,t} + \left(c_p' v_i^* \theta\right)_{,i} = \frac{1}{RePr}\left(k' \theta_{,i}\right)_{,i} + \frac{Ec}{Mm^2\, Rm} \varepsilon_{ijk}\varepsilon_{ilm} H_{k,j}^* H_{m,l}^* + \frac{Ec}{Re} \Phi^{*(i)} \qquad (28)$$

$$H_{,t}^* - \left(v_j H_i^* - v_i H_j^*\right)_{,j} = \frac{1}{Rm} H_{i,jj}^* \qquad (29)$$

where $\Phi^{*(i)}$ is the incompressible flow viscous dissipation function

$$\Phi^{*(i)} = \eta' \left(v_{i,j}^* + v_{j,i}^*\right) v_{i,j}^* \qquad (30)$$

Notice that $c_p \frac{DT}{Dt} = \frac{Dh}{Dt}$. Hence, the rate of change of enthalpy is given as

$$\frac{Dh}{Dt} = h_{,t} + v_i h_{,i} \qquad (31)$$

In the case of a liquid/solid mixture, the enthalpy per unit mass of the mushy region becomes

$$h = c_p T - LS. \tag{32}$$

Then

$$h_{,t} = c_p T_{,t} - LS_{,t} = \left(c_p - L\frac{\partial S}{\partial T}\right)T_{,t} \tag{33}$$

and the convective term of equation (31) can be written as

$$v_i h_{,i} = v_i c_p T_{,i} - v_i LS_{,i} = \left(c_p - L\frac{\partial S}{\partial T}\right) v_i T_{,i} \tag{34}$$

This suggests that we should introduce an equivalent specific heat, $c_{pe} = c_p - L\frac{\partial S}{\partial T}$. Then,

$$c_{pe} = c_{po}\, c_{pe}' = c_{po}\left(c_p' - \frac{L}{c_{po}}\frac{\partial S}{\partial \theta}\frac{d\theta}{dT}\right) \tag{35}$$

Hence, the non-dimensional specific heat coefficient is

$$c_{pe}' = c_p' - \frac{L}{c_{po}\,\Delta T_o}\frac{\partial S}{\partial \theta} \tag{36}$$

where S could be a general nonlinear function of θ [11]. This approach is called the "enthalpy method" [3]. After dropping the asterisk symbol and introducing the non-dimensional equivalent specific heat, c_{pe}', into equations (26-29), they become

$$v_{i,i} = 0 \tag{37}$$

$$v_{i,t} + (v_i v_j)_{,j} = \frac{1}{Re}\left(\eta' v_{i,j}\right)_{,j} - p_{,i} + \frac{1}{Fr^2} g_i - \frac{Gr}{Re^2} g_{,i} + \frac{1}{Mm^2}\varepsilon_{ijk}\varepsilon_{jlm}H_{m,l}H_k \tag{38}$$

$$\left(c_{pe}'\theta\right)_{,t} + \left(c_{pe}' v_i \theta\right)_{,i} = \frac{1}{RePr}\left(k' \theta_{,i}\right)_{,i} + \frac{Ec}{Mm^2 Rm}\varepsilon_{ijk}\varepsilon_{ilm}H_{k,j}H_{m,l} \tag{39}$$

Viscous dissipation can be neglected since an order of magnitude analysis shows that

$$\frac{\rho_o c_{pe}\frac{\partial T}{\partial t}}{\Phi^{(i)}} = \frac{\rho_o c_{pe}\Delta T_o}{\eta_o}\frac{v_o}{l_o}\frac{1}{v_o^2/l_o^2} = \frac{Re}{Ec} \tag{40}$$

For example [12], for $NaNO_3$ with ρ_o = 2000 kg/m^3, c_{po} = 1880 J/(kg-K), η_o = 0.00282 kg/(m-s), this ratio amounts to 1.333 x $10^9\,\Delta T_o l_o/v_o$. Hydrostatic, hydrodynamic, and magnetic field pressure can be combined to give

$$\bar{p} = \rho\,\phi_{,i} + p + \frac{\mu}{2}H_iH_i \tag{41}$$

where φ is defined as $g_i = Fr^2\,\phi_{,i}$. Magnetic force term in the momentum equation can be transformed in the following way

$$\begin{aligned}\varepsilon_{ijk}\varepsilon_{ilm}H_{k,j}H_{m,l} &= \left(\delta_{im}\delta_{kl} - \delta_{il}\delta_{km}\right)H_{m,l}H_k \\ &= H_k\left(H_{i,k} - H_{k,i}\right)\end{aligned} \tag{42}$$

Since $H_{i,i} = 0$, the magnetic field term in the energy equation becomes

$$\begin{aligned}\varepsilon_{ijk}\varepsilon_{ilm}H_{k,j}H_{m,l} &= \left(H_kH_{i,k} + H_{k,k}H_i\right) - H_kH_{k,i} \\ &= \left(H_iH_k\right)_{,k} - H_{,i}^2 \\ &= \left(H_iH_k - \tfrac{1}{2}H^2\delta_{ik}\right)_{,k}\end{aligned} \tag{43}$$

Finally, MHD Navier-Stokes extended Boussinesq equations can be written as

$$v_{i,i} = 0 \tag{44}$$

$$v_{i,t} + \left(v_i v_j\right)_{,j} = \frac{1}{Re}\left(\eta' v_{i,j}\right)_{,j} - \bar{p}_{,i} - \frac{Gr}{Re^2} g_{,i} + \frac{Hr^2}{RmRe} H_k\left(H_{i,k} - H_{k,i}\right) \tag{45}$$

$$\left(c_{pe}'\theta\right)_{,t} + \left(c_{pe}' v_i \theta\right)_{,i} = \frac{1}{RePr}\left(k' \theta_{,i}\right)_{,i}$$

$$+\frac{EcHt^2}{Rm^2Re}\left(H_iH_k - \frac{1}{2}H^2\delta_{ik}\right)_{,k} \qquad (46)$$

and the magnetic transport equations as

$$H_{,t} - \left(v_j H_i - v_i H_j\right)_{,j} = \frac{1}{Rm} H_{i,jj} \qquad (47)$$

NUMERICAL RESULTS

Based on this analytic model a computer program was developed [5,7,8,9] incorporating the logic of explicitly enforcing zero velocity at all grid points where the instantaneous temperature is lower than solidus temperature, while adding the latent heat at all mushy region points where the local instantaneous temperature was between liquidus and solidus. An explicit finite difference algorithm was used in conjunction with boundary conforming curvilinear non-orthogonal coordinate system following a structured computational grid. Time integration was performed using a four-stage Runge-Kutta scheme. No artificial dissipation was used in this work. Details of this numerical analysis have been reported previously [5,8,13].

The following values of physical properties have been obtained from the publications of Duranceau and Brown [14], Sackinger et al. [15] and Mühlbauer et al. [16].

ρ_l [kg m^{-3}]	2550
ρ_s [kg m^{-3}]	2330
C_{pl} [J kg^{-1} K^{-1}]	1059
C_{ps} [J kg^{-1} K^{-1}]	1038
k_l [W m^{-1} K^{-1}]	64
k_s [W m^{-1} K^{-1}]	22
T_l [K]	1685
T_m [K]	1683
T_s [K]	1681
η [kg m^{-1} s^{-1}]	7.018 x 10^{-4}
α [K^{-1}]	1.4 x 10^{-4}
L [J kg^{-1}]	1803000
σ_l [Ω^{-1} m^{-1}]	12.3 x 10^5
σ_s [Ω^{-1} m^{-1}]	4.3 x 10^4
μ [Tm A^{-1}]	4π x 10^{-6}

Table 1. Physical properties for silicon.

The values of the remaining reference parameters were: $v_o = 0.05$ ms^{-1}, $l_o = 0.05$ m, $g_o = 9.81$ m s^{-2}, $T_h = 1715$ K, $T_c = 1621$ K, $T_s = 1681$ K and $T_l = 1685$ K. We have used a simple linear dependence of the solid fraction, S, on temperature, that is, $S = (T_l - T) / (T_l - T_s)$. Hence,

Nondimensional numbers	Values used for silicon melt
$Re = \frac{\rho_o v_o l_o}{\eta_o}$	8300.08
$Fr = \frac{v_o}{(g_o l_o)^{1/2}}$	0.071392
$Gr = \frac{\rho_o^2 \alpha_o g_o l_o^3 \Delta T_o}{\eta_o^2}$	56.769 x 10^6
$Ec = \frac{v_o^2}{c_{po} \Delta T_o}$	7.869 x 10^{-8}
$Pr = \frac{\eta_o c_{po}}{k_o}$	0.0116
$Pm = \frac{\mu_o \sigma \eta_o}{\rho_o}$	4.44 x 10^{-6}
$Ht = \mu_o l_o H_o \left(\frac{\sigma}{\eta_o}\right)^{1/2}$	2093 B_o

Table 2. Nondimensional parameters.

Notice that we have assumed that the magnetic permeability coefficient for silicon is one order of magnitude larger than for vacuum. Consequently, the Hartmann number in our case becomes $Ht = 2093\ B_o$, where B_o is the magnetic field strength measured in Teslas. It should also be pointed out that the values of C_p, k and η were varied linearly within the mushy region.

We chose to analyze a solidification process inside a rectangular container with a width-to-height ratio of 3:1 filled with molten silicon. It was subjected to a uniformly high temperature, $T_h > T_l$, along the bottom wall and a uniformly cold temperature, $T_c < T_s$, along the upper wall. Vertical walls were thermally insulated. This configuration corresponds to a typical solidification process in which the cooling front propagates from above

[17]. The entire domain was discretized with a clustered computational grid consisting of 60 x 60 grid cells. A very small amount of fourth order artificial dissipation was used in order to prevent even-odd coupling that is characteristic of central difference schemes. Artificial compressibility method was used [5] with the artificial compressibility coefficient in the mass conservation having a value $\beta = 10^4$. A CFL number of 2.8 corresponding to the maximum allowable value for the four step Runge-Kutta scheme was used together with a von Neumann number of the order 0.001. The gravitational acceleration vector pointed vertically downward as was the case with the uniform magnetic field vector.

The first test case involved no magnetic field and 100% of gravity. The velocity vector plot (Fig. 1a) and streamline pattern (Fig. 1b) indicate the existance of two recirculation zones. The isotherms (Fig. 1c) demonstrate the recirculation in the molten silicon does not influence the solid/liquid interface shape.

The second test case involved a uniform magnetic field having a strength of 1 Tesla and 100% gravity. Figures 2a and 2b indicate that the recirculation vortices have migrated towards the side walls, while the isotherms (Fig. 2c) demonstrate a deformation of the solid/liquid interface due to the presence of the magnetic field. By comparing Figure 1c and Figure 2c, it is obvious that the amount of accrued solid phase is significantly lower in the case with the strong magnetic field. This is caused by the Joule heating effect generated by the induced electric current inside the melt and should not be discarded as insignificant when analyzing solidification. This fact was also confirmed in the recent publications by Salcudean [18,19].

The third test case involved no magnetic field while gravity was reduced to 1% resulting in a reduction of Grashoff number by two orders of magnitude. Figure 3a indicates a considerably weaker recirculation in the melt which is reconfirmed by the streamline pattern (Fig. 3b). It is interesting to notice that the amount of accrued solid and the corresponding isotherms (Fig. 3c) for this low-gravity test case are practically identical to Figure 1c which is obtained in the case with 100% gravity.

Isotherms were plotted in intervals of $\Delta T = 3$ K. Convergence histories for these three runs are displayed in Figure 4 indicating that the solidification of silicon with a strong magnetic field proceeds at a significantly slower rate because of the Joule heating effect, while micro-gravity has a negligible effect on the solidification of this material.

CONCLUSIONS

A complete analytic model has been derived for a multidimensional solidification simulation under the influence of an externally applied steady magnetic field. The Boussinesq approximation was expanded to incorporate temperature dependent physical properties. A computer program was developed and tested on a two-dimensional closed container filled with molten silicon. Computational results confirm that the magnetic field has a profound influence on the flow field by reducing the strength of flow recirculation regions and causing deformation of the solid-liquid interface. In addition, it was found that the amount of the accrued solidified phase diminishes with the increase of the magnetic field strength due to additional heat generated inside the melt as a consequence of the Joule heating effect.

ACKNOWLEDGEMENTS

The authors would like to express their gratitude to Cray Research, Eagan, Minnesota for providing the computing facilities and for the support of the second author's internship. Special thanks are also due to Mr. Scott Sheffer for his help in the preparation of the final version of this paper and to Apple Computer, Inc. for their donated post-processing equipment

REFERENCES

1. Tzavaras, A. A. and Brody, H. D., "Electromagnetic Stirring and Continuous Casting - Achievements, Problems and Goals", Journal of Metals, March, 1984, pp. 31-37.
2. Tseng, A. A.,"Electroheating Modeling In Metal Processing: A Review", Adv. Eng. Software, Vol.10, No.2, 1988, pp. 58-71.
3. Poirier, D. and Salcudean, M., "On Numerical Methods Used in Mathematical Modeling of Phase Change in Liquid Metals", ASME paper 86-WA/HT-22, Anaheim, CA, December 7-12, 1986.
4. Jeffrey, A., "Magnetohydrodynamics," University Mathematical Texts, 33, Oliver & Royd LTD, Edinburgh, U. K., 1966.
5. Lee,S. and Dulikravich,G.S.,"Magnetohydrodynamic Flow Computations in Three Dimensions", AIAA

Paper 91-0388. Aerospace Sciences Meeting, Reno, NV, January 7-10, 1991; also to appear in Int. J. of Numerical Methods in Fluids, summer 1991.

6. Stuetzer, O. M., "Magnetohydrodynamics and Electrohydrodynamics," The Physics of Fluids, Vol. 5, No. 5, May 1962, pp. 534-544.
7. Lee, S., Dulikravich, G.S. and Kosovic, B.,"Interaction of Magnetic Field With Blood Flow", Proceedings of the 17th Annual Northeast Bioengineering Conf., Univ. of Connecticut, Hartford, CT, April 4-5, 1991.
8. Lee, S. and Dulikravich, G.S.,"Computation of Magnetohydrodynamic Flows With Joule Heating and Buoyancy", Proc. of the Internat. Aerospace Congress, Melbourne, Australia, May 12-16, 1991.
9. Dulikravich, G.S., Kosovic, B. and Lee, S.,"Solidification of Variable Property Melts in Closed Containers: Magnetic Field Effects", Proceedings of the 13th IMACS World Congress on Computation and Applied Mathematics, Trinity College, Dublin, Ireland, July 22-26, 1991.
10. Gray, D. D. and Giorgini, A., "The Validity of the Boussinesq Approximation for Liquids and Gases", Int. J. Heat and Mass Transfer, Vol. 19, 1976, pp. 545-551.
11. Storti, M., Crivelli, L. A. and Idelsohn, S. R., "An Efficient Tangent Scheme for Solving Phase-Change Problems", Comp. Meth. in Appl. Mech. and Eng., Vol. 66, 1988, pp. 65-86.
12. Lan, C. W. and Kou, S., "Heat Transfer, Fluid Flow and Interface Shapes in Floating-Zone Crystal Growth," Journal of Crystal Growth, Vol. 108, 1991, pp. 351-366.
13. Lee, S. and Dulikravich, G. S., "Accelerated Computation of Viscous Incompressible Flows With Heat Transfer", Proc. of First Int. Conf. Exp. Comput. Aerothermodynamics of Internal Flows, ed: Chen, N.-X., Beijing, PR China, July 7-11, 1990; also Numerical Heat Transfer B: Fundamentals, Vol. 19, June 1991, pp. 223-241.
14. Duranceau, J. L. and Brown, R. A., "Thermal-Capillary Analysis of Small-Scale Floating Zones: Steady-State Calculations," Journal of Crystal Growth, Vol. 75, 1986, pp. 367-389.
15. Sackinger, P. A., Brown, R. A. and Derby, J. J., "A Finite Element Method for Analysis of Fluid Flow, Heat Transfer and Free Interfaces in Czochralski Crystal Growth," International Journal for Numerical Methods in Fluids, Vol. 9, 1989, pp. 453-492.
16. Mühlbauer, A., Erdmann, W. and Keller, W., "Electrodynamic Convection in Silicon Floating Zones," Journal of Crystal Growth, Vol. 64, 1983, pp. 529-545.
17. Kerr, R. C., Woods, A. W., Worster, M. G., and Huppert, H. E., " Solidification of an Alloy Cooled From Above. Part 1. Equilibrium Growth," Journal of Fluid Mechanics, Vol. 216, 1990, pp. 323-342.
18. Sabhapathy, P. and Salcudean, M., "Numerical Study of Flow and Heat Transfer in LEC Growth of GaAs with an Axial Magnetic Field," Journal of Crystal Growth, Vol.104, 1990, pp. 371-388.
19. Salcudean, M. and Sabhapathy, P., "Numerical Study of Liquid Encapsulated Czochralski Growth of Gallium Arsenide with and without an Axial Magnetic Field," ASME MD - Vol. 20, Computer Modeling and Simulation of Manufacturing Processes, Editors: Singh, B., Im, Y. T., Haque, I. and Altan, C., Book No. G00552, 1990,.pp.115-127.

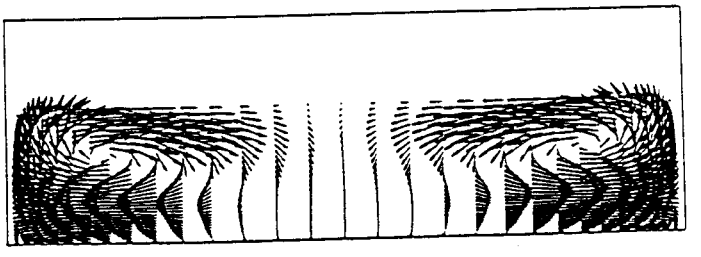

Figure 1a. Velocity vector profiles: 100% gravity and no magnetic field.

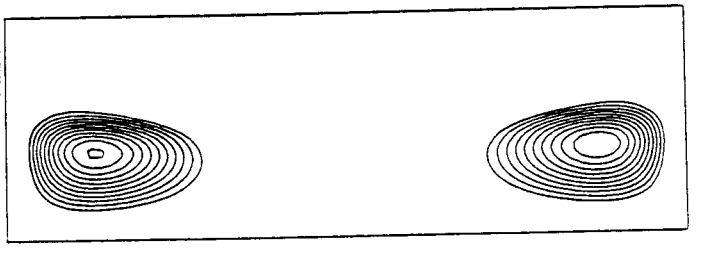

Figure 1b. Streamlines: 100% gravity and no magnetic field.

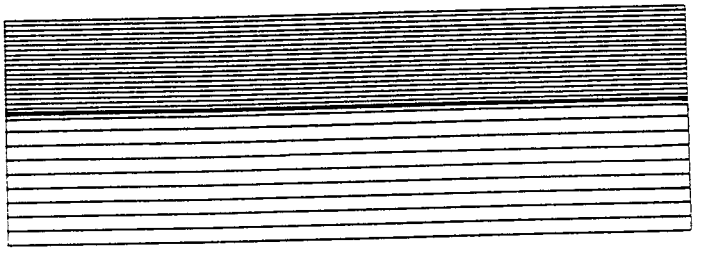

Figure 1c. Isotherms: 100% gravity and no magnetic field.

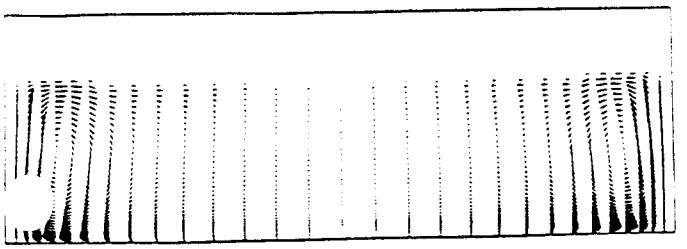

Figure 2a. Velocity vector profiles: 100% gravity and 1 Tesla uniform magnetic field imposed.

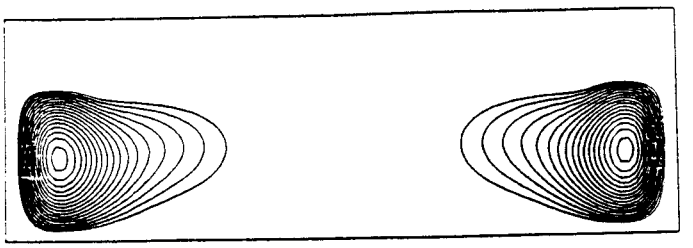

Figure 2b. Streamlines: 100% gravity and 1 Tesla uniform magnetic field imposed.

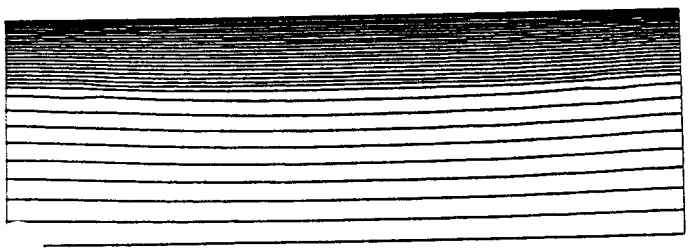

Figure 2c. Isotherms: 100% gravity and 1 Tesla uniform magnetic field imposed.

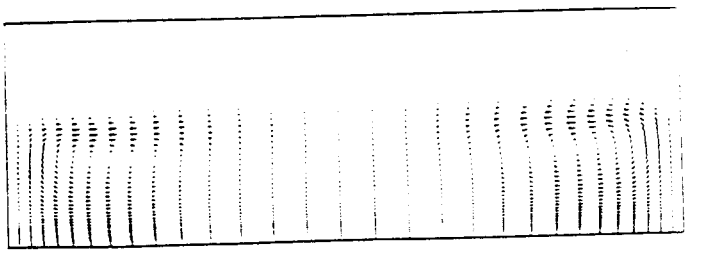

Figure 3a. Velocity vector profiles: 1% gravity and no magnetic field.

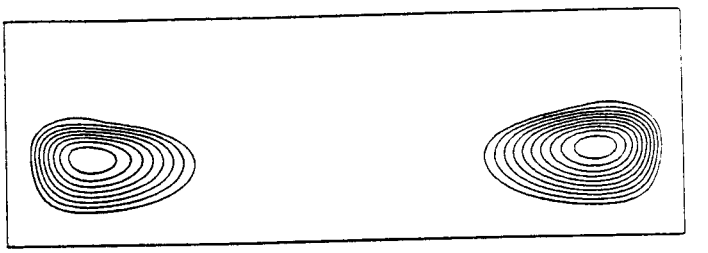

Figure 3b. Streamlines: 1% gravity and no magnetic field.

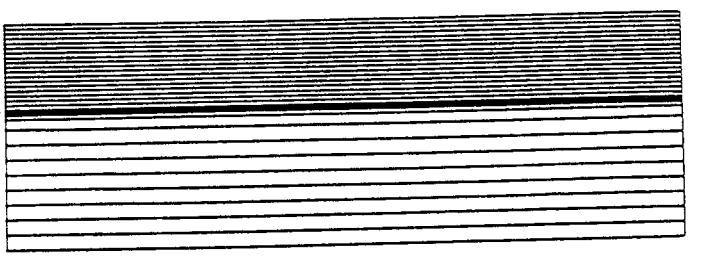

Figure 3c. Isotherms: 1% gravity and no magnetic field.

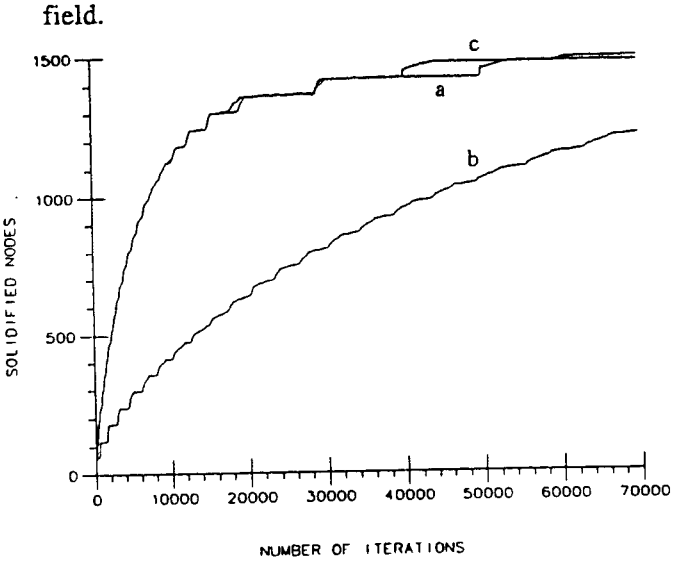

Figure 4. Convergence histories for the three examples. a) 100% gravity and no magnetic field, b) 100% gravity and 1 Tesla magnetic field, c) 1% gravity and no magnetic field.